Supporting Information:

Measurement of vaporization enthalpy by isothermogravimetrical method and prediction of the polarity for 1-alkyl-3-methylimidazolium acetate {[C$_n$mim][OAc] (n = 4, 6)} ionic liquids

Jie Wei, Xiaoxue Bu, Wei Guan*, Nannan Xing, Dawei Fang and Yang Wu*

Section A ^{1}H NMR spectra

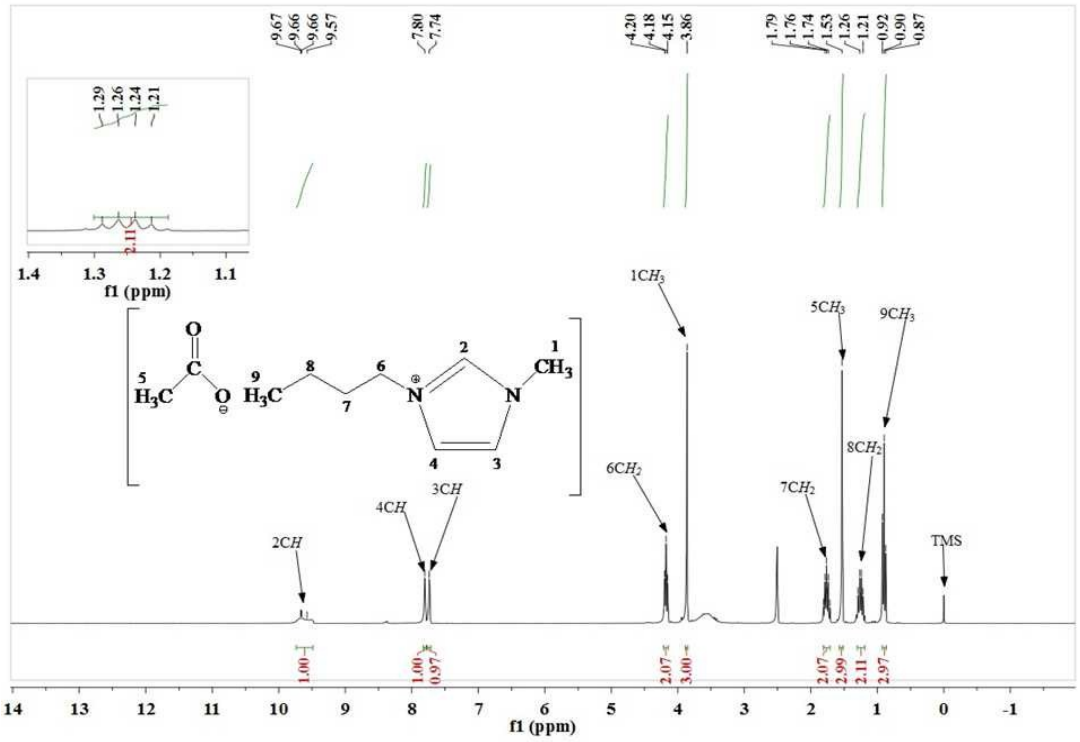

Fig. S1 ^{1}H NMR spectrum δ_H (300 MHz, DMSO) of [C$_4$mim][OAc]

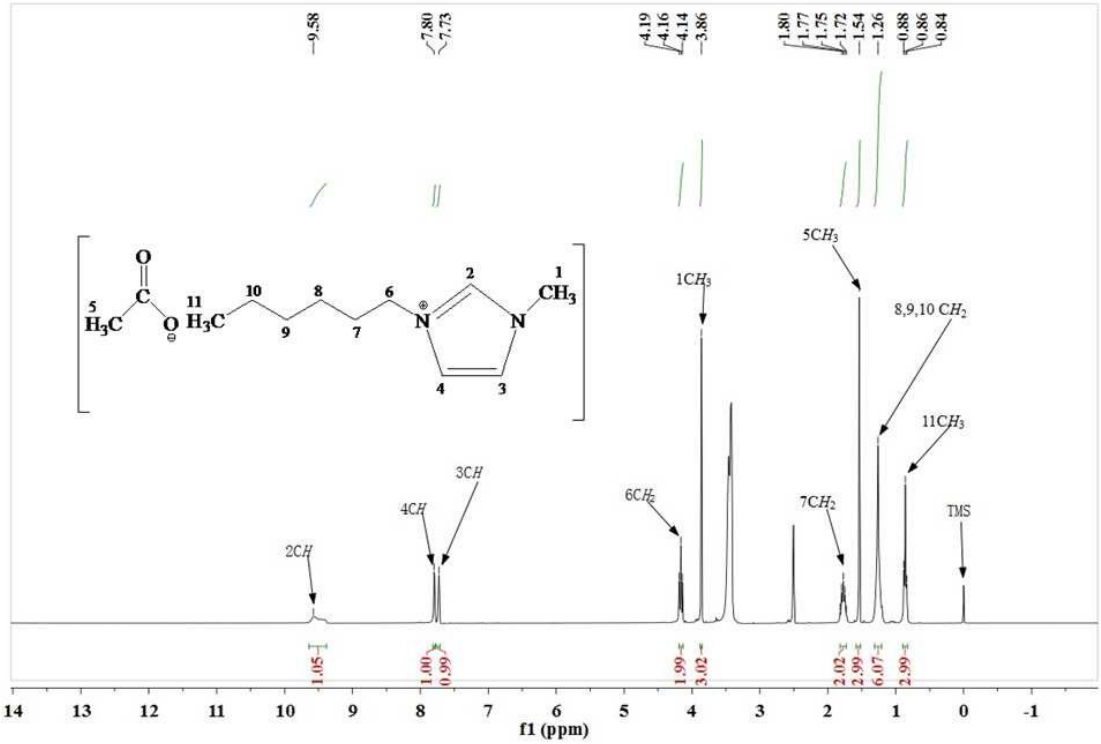

Fig. S2 ^{1}H NMR spectrum δ_{H} (300 MHz, DMSO) of [C_6mim][OAc]

Section B Thermal analysis

Calorimetric data were obtained with a differential scanning calorimeter DSC (Mettler-Toledo Co., Switzerland). The temperature range was – 100-100 °C with heating rate of 10 °C·min^{-1}. Then samples were incubated at – 100 °C for 5 min and were then heated to 100 °C.

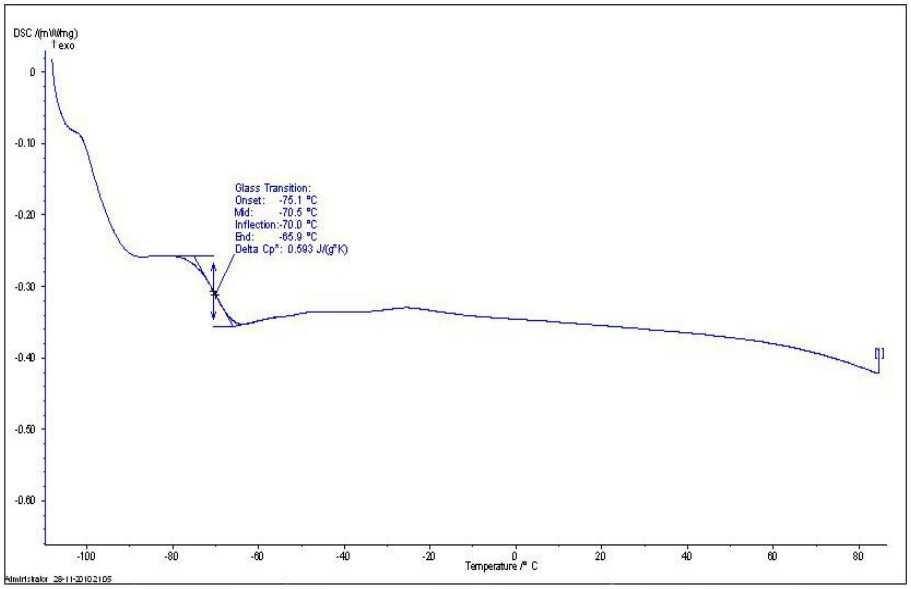

Fig. S3 DSC thermogram of [C_4mim][OAc]

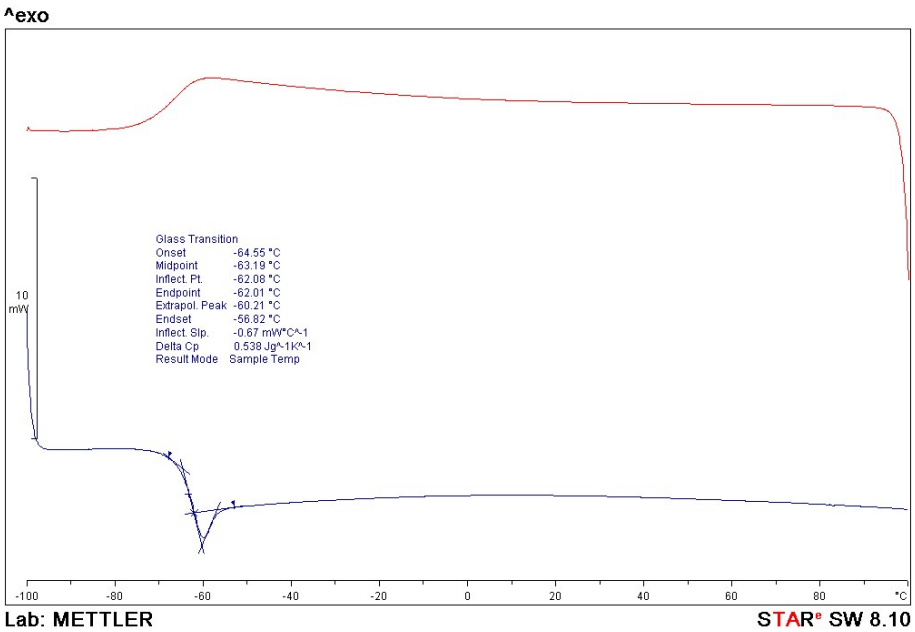

Fig. S4 DSC thermogram of [C_6mim][OAc]

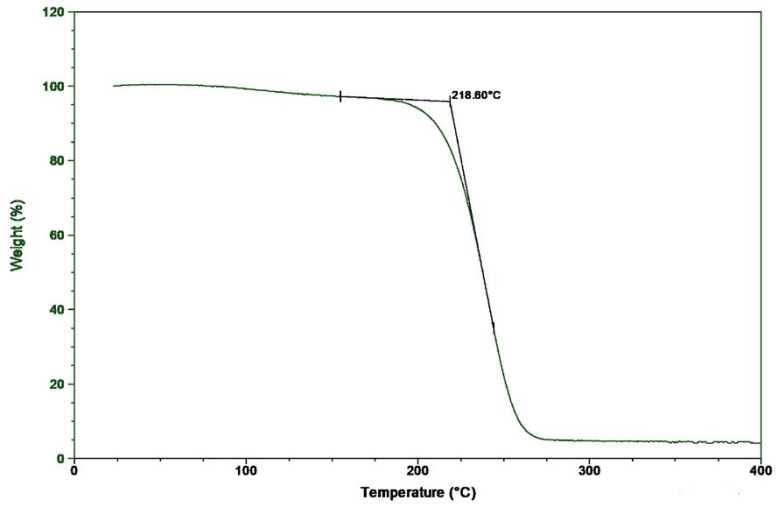

Fig. S5 TG plot of [C_4mim][OAc]

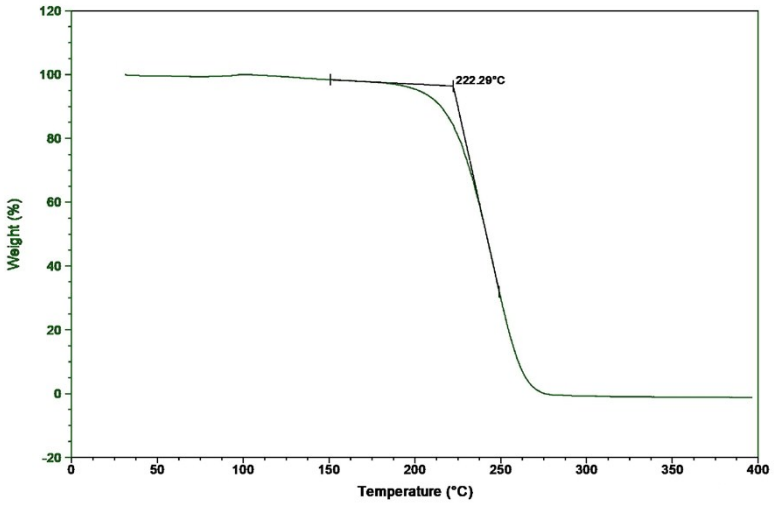

Fig. S6 TG plot of [C_6mim][OAc]

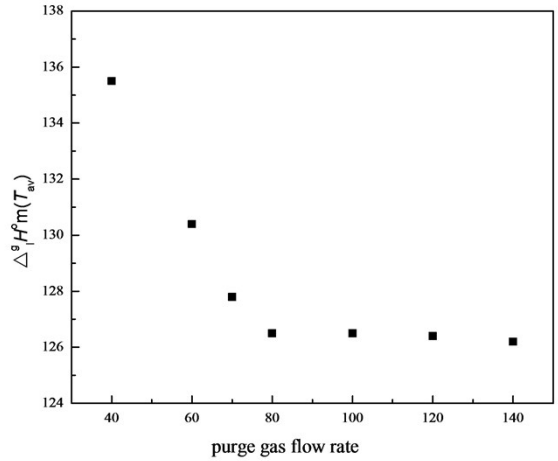

Fig. S7 The influence of purge gas rate on the evaporation enthalpy: Nitrogen flow of 40, 50, 60, 70, 80, 100, 120 and 140 mL·min^{-1} of [C_4mim][OAc] at the same temperature and hold period in the experiments.

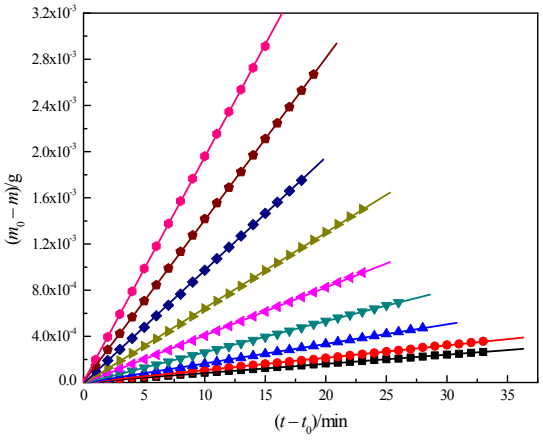

Fig.S8 Plot of $(m_0 - m)$ *vs.* $(t - t_0)$ for[C_4mim][OAc] at the temperature rang from 408 K to 448 K.

■408K: $m_0 - m = -1.924 \times 10^{-6} + 7.982 \times 10^{-6}(t - t_0)$, $r = 0.9998$, $s = 1.70 \times 10^{-6}$;

●413K: $m_0 - m = -7.048 \times 10^{-7} + 1.074 \times 10^{-5}(t - t_0)$, $r = 0.9998$, $s = 2.00 \times 10^{-6}$;

▲418K: $m_0 - m = -4.465 \times 10^{-6} + 1.694 \times 10^{-5}(t - t_0)$, $r = 0.9999$, $s = 2.19 \times 10^{-6}$;

▼423K: $m_0 - m = -6.541 \times 10^{-6} + 2.687 \times 10^{-5}(t - t_0)$, $r = 0.9999$, $s = 2.66\times 10^{-6}$;

◀428K: $m_0 - m = -6.589 \times 10^{-6} + 4.147 \times 10^{-5}(t - t_0)$, $r = 0.9999$, $s = 2.88\times 10^{-6}$;

▶433K: $m_0 - m = -1.154 \times 10^{-5} + 6.549 \times 10^{-5}(t - t_0)$, $r = 0.9999$, $s = 5.14 \times 10^{-6}$;

◆438K: $m_0 - m = -7.777 \times 10^{-6} + 9.794 \times 10^{-5}(t - t_0)$, $r = 0.9999$, $s = 5.08 \times 10^{-6}$;

⬟443K: $m_0 - m = 3.551 \times 10^{-6} + 1.403 \times 10^{-4}(t - t_0)$, $r = 0.9999$, $s = 4.38 \times 10^{-6}$;

⬢448K: $m_0 - m = 7.937 \times 10^{-6} + 1.946 \times 10^{-4}(t - t_0)$, $r = 0.9999$, $s = 6.50 \times 10^{-6}$.

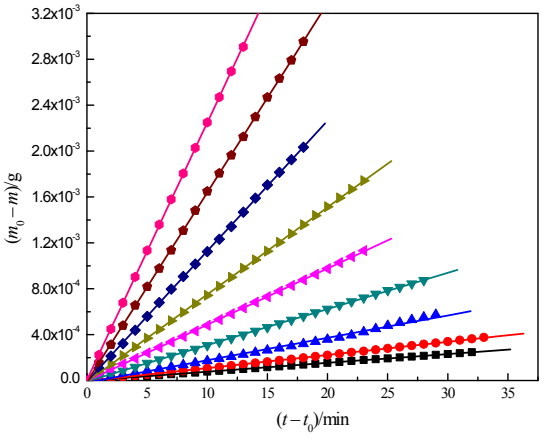

Fig.S9 Plot of $(m_0 - m)$ *vs.* $(t - t_0)$ for[C_6mim][OAc] at the temperature rang from 408 K to 448 K.

408K: $m_0 - m = -4.853 \times 10^{-7} + 7.707 \times 10^{-6}(t - t_0)$, $r = 0.9999$, $s = 3.77 \times 10^{-7}$;

413K: $m_0 - m = -5.987 \times 10^{-6} + 1.143 \times 10^{-5}(t - t_0)$, $r = 0.9998$, $s = 2.51 \times 10^{-6}$;

418K: $m_0 - m = -1.813 \times 10^{-5} + 1.950 \times 10^{-5}(t - t_0)$, $r = 0.9992$, $s = 1.31 \times 10^{-5}$;

423K: $m_0 - m = -8.098 \times 10^{-6} + 3.158 \times 10^{-5}(t - t_0)$, $r = 0.9999$, $s = 2.73 \times 10^{-6}$;

428K: $m_0 - m = -5.263 \times 10^{-6} + 4.907 \times 10^{-5}(t - t_0)$, $r = 0.9999$, $s = 3.49 \times 10^{-6}$;

433K: $m_0 - m = -1.124 \times 10^{-5} + 7.606 \times 10^{-5}(t - t_0)$, $r = 0.9999$, $s = 4.25 \times 10^{-6}$;

438K: $m_0 - m = -9.766 \times 10^{-6} + 1.137 \times 10^{-4}(t - t_0)$, $r = 0.9999$, $s = 7.44 \times 10^{-6}$;

443K: $m_0 - m = -1.009 \times 10^{-5} + 1.648 \times 10^{-4}(t - t_0)$, $r = 0.9999$, $s = 6.12 \times 10^{-6}$;

448K: $m_0 - m = 4.534 \times 10^{-6} + 2.242 \times 10^{-4}(t - t_0)$, $r = 0.9999$, $s = 5.96 \times 10^{-6}$.

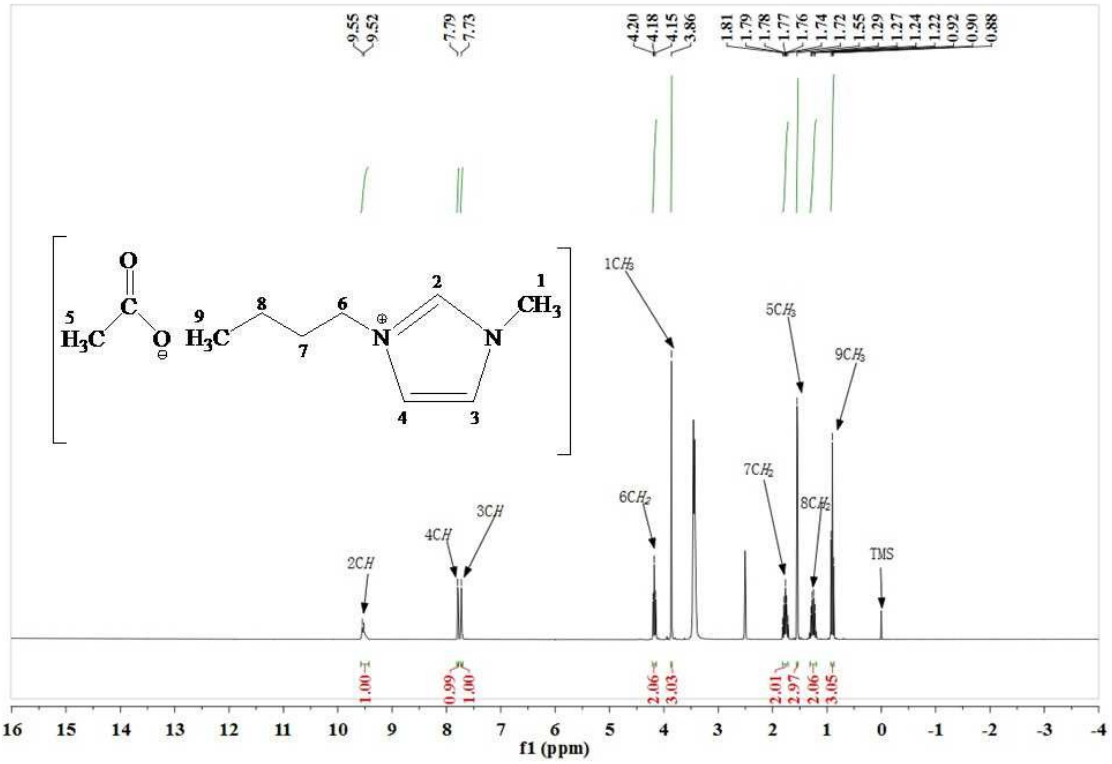

Fig. S10 The ^{1}H NMR spectrum δ_H (300 MHz, DMSO) of residual [C_4mim][OAc] in the crucible

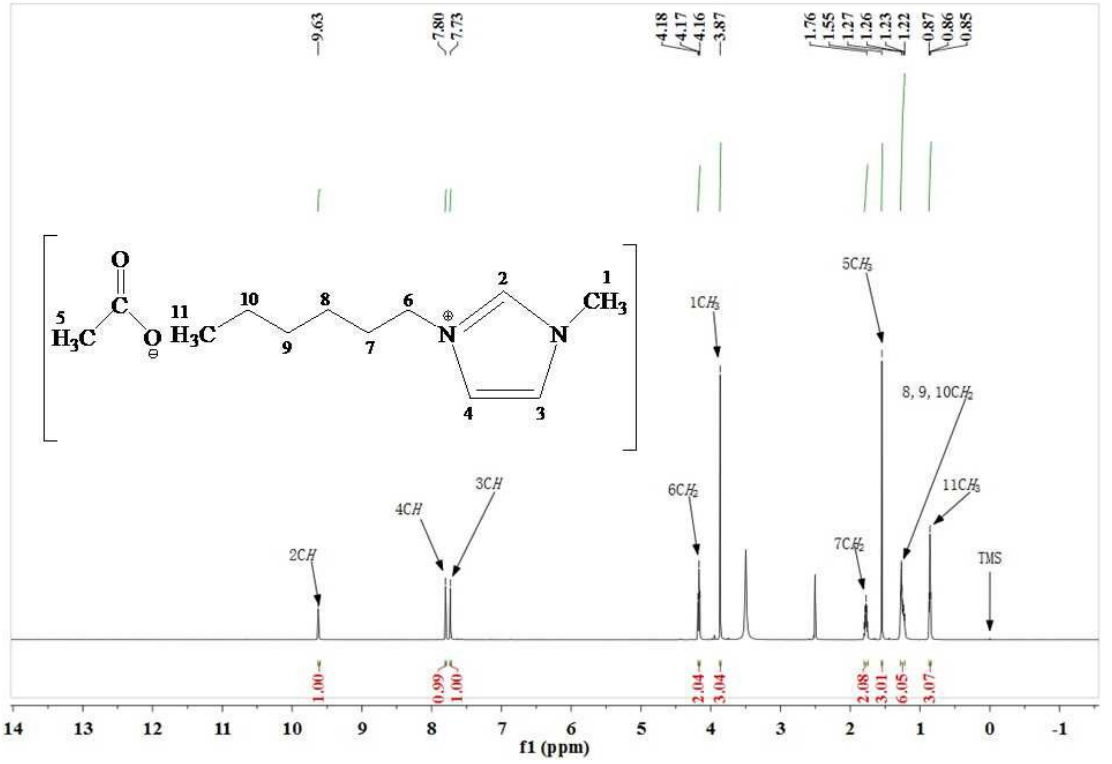

Fig. S11 The ^{1}H NMR spectrum δ_H (300 MHz, DMSO) of residual [C_6mim][OAc] in the crucible

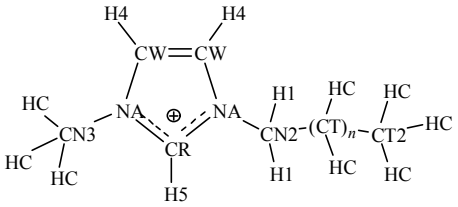

$[C_n\text{mim}]^+(n = 2,4)$

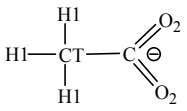

$[\text{OAc}]^-$

Fig. S12 Schematic structure and atomic type notations of the 1-alkyl-3-methylimidazolim cation ($[C_n\text{mim}]^+$) (n = 4, 6), and acetic acid anion ($[\text{OAc}]^-$) in the AMBER force field.

Table S1 The source and purity of the materials.

Chemical name	Source	Purification method	Mass fraction purity
N-methylimidazole	ACROS	Further purification	≥ 0.998
Acetic acid	Shanghai Reagent Co. Ltd.	Further purification	≥ 0.990
1-bromobutane	Shanghai Reagent Co. Ltd.	Further purification	> 0. 985
1-chlorohexane	Shanghai Reagent Co. Ltd.	Further purification	> 0. 985
Ethyl acetate	Shanghai Reagent Co. Ltd.	No further purification	> 0.985
Acetonitrile	Shanghai Reagent Co. Ltd.	No further purification	> 0.995
Anion-exchange resin (type 717)	Shanghai Reagent Co. Ltd.	No further purification	granularity: > 0.950

Table S2 The values of $-\mathrm{d}m/\mathrm{d}t$ and $\ln[T^{1/2}\cdot(-\mathrm{d}m/\mathrm{d}t)]$ for $[C_n\mathrm{mim}][\mathrm{OAc}]$($n$ = 4,6) from 408 K to 448 K.

T[a]/K	T^{-1} /K^{-1}	$10^5(-\mathrm{d}m/\mathrm{d}t)$ /g·min^{-1}	$\ln[T^{1/2}\cdot(-\mathrm{d}m/\mathrm{d}t)]$
		$[C_4\mathrm{mim}][\mathrm{OAc}]$	
408	0.002451	0.7982	– 8.733
413	0.002421	1.074	– 8.429
418	0.002392	1.694	– 7.968
423	0.002364	2.687	– 7.501
428	0.002336	4.147	– 7.061
433	0.002309	6.549	– 6.598
438	0.002283	9.794	– 6.190
443	0.002257	14.03	– 5.824
448	0.002232	19.46	– 5.492
		$[C_6\mathrm{mim}][\mathrm{OAc}]$	
408	0.002451	0.7707	– 8.768
413	0.002421	1.143	– 8.368
418	0.002392	1.950	– 7.827
423	0.002364	3.158	– 7.339
428	0.002336	4.907	– 6.893
433	0.002309	7.606	– 6.449
438	0.002283	11.37	– 6.041
443	0.002257	16.48	– 5.664
448	0.002232	22.42	– 5.351

[a]: the standard uncertainty (0.68 level of confidence): $u(T)$ = 0.02 K for temperature.

The details of the new estimation values of $\Delta^g_l C_p^o{}_m$ based on statistical thermodynamics and some auxiliary experimental data.

Heat capacities in the liquid and gaseous state could be considered as the sum of translational, rotational, vibrational, and conformational contributions according to equations (1) and (2).

$$C_p^o{}_m(g) = C_v^o{}_m\,(\text{transl, g}) + C_v^o{}_m\,(\text{rot, g}) + C_v^o{}_m\,(\text{vib, g}) + C_v^o{}_m\,(\text{conf, g}) + (C_p^o{}_m - C_v^o{}_m)_g \qquad (1)$$

$$C_p^o{}_m(l) = C_v^o{}_m\,(\text{transl, l}) + C_v^o{}_m\,(\text{rot, l}) + C_v^o{}_m\,(\text{vib, l}) + C_v^o{}_m\,(\text{conf, l}) + (C_p^o{}_m - C_v^o{}_m)_l \qquad (2)$$

where $(C_p^o{}_m - C_v^o{}_m)_g$ and $(C_p^o{}_m - C_v^o{}_m)_l$ are the appropriate differences between isobaric and isochoric heat capacities. With assumption that vibrational contributions, as well as that equilibrium of conformers are not significantly different in the gas and in the liquid phase, we have combined equations (1) and (2) and suggested for the heat capacity difference between gas and liquid the following simplified expression:

$$\Delta^g_l C_p^o{}_m = C_v^o{}_m\,(\text{transl, g}) + C_v^o{}_m\,(\text{rot, g}) + (C_p^o{}_m - C_v^o{}_m)_g - C_v^o{}_m\,(\text{transl, l}) - C_v^o{}_m(\text{rot, l}) - (C_p^o{}_m - C_v^o{}_m)_l \qquad (3)$$

From the common statistical thermodynamics knowledge, a sum of contributions of the free rotation of a molecule and free translational motion of a molecule into the heat capacity in the ideal gas state is equal to 3 *R*. According to the oscillation theory[1] in the condensed state no free rotation of the molecule or linear motion of the molecules is possible. So the translational motion is converted into the vibrations with low frequencies and the rotation is converted into the librations or hindered rotation. The contribution of vibrations (librations) at low frequencies into the heat capacity is *R* for each degree of freedom (6 *R* for all converted rotational and translational contributions). In the case of hindered rotation this contribution will get within (1/2) *R* to *R* for each degree of hindered rotation freedom. In the case of highly viscous liquids with quasi-crystal structure the value of 3 *R* (vibrations) is more possible than (3/2) *R* (free motion). With the $(C_p^o{}_m - C_v^o{}_m)_g = R$ for ideal gas systems equation (3) was simplified as follows:

$$\Delta^g_l C_p^o{}_m = (3/2)\,R + (3/2)\,R + R - 3R - 3R - (C_p^o{}_m - C_v^o{}_m)_l = -2\,R - (C_p^o{}_m - C_v^o{}_m)_l \qquad (4)$$

It is apparent now that the contribution $(C_p^o{}_m - C_v^o{}_m)_l$ in equation (4) is the main part of the heat capacity difference, $\Delta^g_l C_p^o{}_m$, vitally important for the proper temperature adjustments of vaporization enthalpies as discussed above. Fortunately, the contribution $(C_p^o{}_m - C_v^o{}_m)_l$ could be easily calculated from the volumetric properties[2]:

$$(C_p^{o}{}_m - C_v^{o}{}_m)_l = (\alpha_p^2/\kappa_T)\, V_m T \quad (5)$$

where α_p is the thermal expansion coefficient, K^{-1}; κ_T is the isothermal compressibility, Pa^{-1}, and V_m is the molar volume, $m^3 \cdot mol^{-1}$. The molar volume, as well as thermal expansion coefficient is usually derived from the liquid density temperature dependence measurements. The compressibility values can be calculated from the pressure dependence of density in the isothermal conditions. But more often the κ_T value is calculated from the speed of sound $W(T, p)$[3]:

$$\kappa_T = (1/\rho)\,(1/W^2 + T\alpha_p^2 M/C_p^{o}{}_m) \quad (6)$$

where ρ is the density of the IL, $kg \cdot m^{-3}$, and M is the molar mass, $kg \cdot mol^{-1}$. Thus, equation (4) developed in this study in combination with equations (5) and (6) could help to assess the value of the heat capacity difference, $\Delta^g_l C_p^{o}{}_m$, provided that volumetric data (ρ, α_p, κ_T) for the IL of interest is available in the literature or estimated with any empirical rules available, e.g. for $W(T, p)$ and $C_p^{o}{}_m(l)$. The speed of sound in the IL $W(T, p)$ could be derived with the help of Auerbach relation [4]:

$$W\,(m/s) = [\sigma/(6.3\times10^{-10}\rho)]^{2/3} \quad (7)$$

where values for density ρ, $kg \cdot m^{-3}$, and surface tension σ, $J \cdot m^{-2}$, were available from the literature [5]. The heat capacity of the liquid phase $C_p^{o}{}_m$ (l) used in equation (6) for calculation of the compressibility κ_T could be estimated using an empirical equation[6]:

$$C_p^{o}{}_m = 8.6 + 1.915\, V_m \quad (8)$$

where V_m is molar volume, $cm^3 \cdot mol^{-1}$. According to above equations, $\Delta^g_l C_p^{o}{}_m$ of the three ILs were calculated. The data needed in the calculation[5] and the values of $\Delta^g_l C_p^{o}{}_m$ are listed in Table .

1 E.A. Moelwyn-Hughes, Physical Chemistry. New York, London, Paris: Pergamon Press, 1954.

2 Y.U. Paulechka, D.H. Zaitsau, G.J. Kabo. *J. Mol. Liq.*, 2004, **115**. 105–111.

3 D.H. Zaitsau, K. Fumino, V.N. Emel'yanenko, A.V. Yermalaeu, R. Ludwig, S.P. Verevkin. *ChemPhysChem*, 2012, **13**, 1868–1876.

4 R. Auerbach, Experientia, 1948, **4**, 473

5 X.X. Ma, J. Wei, Q.B. Zhang, F. Tian, Y.Y. Feng, W. Guan, *Ind. Eng. Chem. Res.*, 2013, **52**, 9490−9496.

6 Y.U. Paulechka, A.G. Kabo, A.V. Blokhin, G.J. Kabo, M.P. Shevelyova, *J. Phys. Chem. Ref. Data*, 2010, **39** 033108

Table The data needed in the calculation of $\Delta^g_l C_p^{o}{}_m$ / $J \cdot K^{-1} \cdot mol^{-1}$ for [C$_n$mim][OAc] (n = 4, 6) and the result at T = 298 K.

ILs	M / $kg \cdot mol^{-1}$	ρ / $kg \cdot m^{-3}$	σ /$J \cdot m^{-2}$	$10^4 V_m$ / $m^3 \cdot mol^{-1}$	$10^4 \alpha_p$ / K^{-1}
[C_4mim]	0.198264	1047.4	0.0354	1.89292	5.84
[OAc]	$10^{10}\kappa_T$/Pa^{-1}	W/$m \cdot s^{-1}$	$C_p^{o}{}_m$(l) / $J \cdot K^{-1} \cdot mol^{-1}$	$\Delta^g_l C_p^{o}{}_m$	

			(Paulechka's)	/J·K^{-1}·mol^{-1}	
	1.32068	1422.44	354.77	-53.4	
	M / kg·mol^{-1}	ρ / kg·m^{-3}	σ /J·m^{-2}	$10^4V_{\mathbf{m}}$ /m^3·mol^{-1}	$10^4\alpha_p$ / K^{-1}
	0.226316	1017.0	0.0331	2.22533	5.99
[C_6mim][OAc]	$10^{10}\kappa_T$ / Pa^{-1}	W / m·s^{-1}	$C_p^{o}{}_m$(l) / J·K^{-1}·mol^{-1} (Paulechka's)	$\Delta^g_l C_p^{o}{}_m$ /J·K^{-1}·mol^{-1}	
	1.1499	1387.11	417.23	-58.7	

Table S3 RESP charge parameters for $[C_n mim]^+$ (n = 4, 6) and $[OAc]^-$ ILs used in this work.

	Atom type	Number	charge	Atom type	Number	charge
$[C_4mim]^+$	NA	150	0.1216	H5	175	0.2251
	CN3	16	-0.1475	H4	173	0.2192
	HC	227	0.1217	H4	190	0.2501
	CN2	351	-0.1322	CT	25	0.1099
	H1	512	0.0916	HC	185	-0.0135
	NA	187	0.0677	CT	28	0.1321
	CR	174	0.0075	HC	201	-0.0052
	CW	172	-0.1232	CT2	21	-0.2353
	CW	204	-0.2058	HC	168	0.0666
$[C_6mim]^+$	NA	150	0.046955	H4	190	0.245614
	CN3	16	-0.166878	CT	25	0.179550
	HC	227	0.127579	HC	185	-0.028410
	CN2	351	-0.085534	CT	28	-0.006660
	H1	512	0.087393	HC	201	0.003158
	NA	187	0.052111	CT	33	-0.046146
	CR	174	0.045611	HC	239	0.010154
	CW	172	-0.106346	CT	35	0.166622
	CW	204	-0.187287	HC	36	-0.024930
	H5	175	0.218411	CT2	21	-0.181556
	H4	173	0.212914	HC	168	0.045050
$[OAc]^-$	O2	505	-0.865	H1	518	0.014
	C	3	0.964	O2	511	-0.873
	CT	23	-0.269			

Table S4 Force field parameters for [$C_n$mim][OAc] (n = 4, 6) ILs used in this work.

	Bonds				
	K_r (kJ·mol^{-1}·Å^{-2})	r_0 (Å)		K_r (kJ·mol^{-1}·Å^{-2})	r_0 (Å)
CT-CT	1297	1.53	CT-CT2	1297	1.53
CT-CN2	1297	1.53	CN3-HC	1423	1.08
CT-HC	1423	1.08	CT2-HC	1423	1.08
CN3-NA	1172	1.47	CN2-N1	1423	1.08
CW-H4	1611	1.07	CR-H5	1590	1.07
CR-NA	1674	1.33	CW-NA	1506	1.38
CN2-NA	1172	1.47	CW-CW	1715	1.34
CT-C	1326	1.53	C-O2	2092	1.25
CT-H1	1423	1.09			
	Angles				
	K_r (kJ·mol^{-1}·Å^{-2}	θ_0 (deg)		K_r (kJ·mol^{-1}·Å^{-2}	θ_0 (deg)
CT-CN2-H1	159	109.5	CT-CT-HC	155	109.5
CT-CT2-HC	155	109.5	CN2-CT-HC	155	109.5
CT2-CT-HC	155	109.5	CT-CT-CT2	167	109.5
CT-CT-CT	167	109.5	CT-CT-CN2	167	109.5
HC-CT-HC	142	109.5	HC-CT2-HC	142	109.5
HC-CN3-NA	230	109.5	CT-CN2-NA	293	112.2
H1-CN2-H1	146	109.5	HC-CN3-HC	142	109.5
H1-CN2-NA	230	109.5	CW-NA-CN3	209	125.7
CW-NA-CN2	209	125.7	CR-NA-CN3	209	126.3
CR-NA-CN2	209	126.3	CW-CW-NA	502	107.0
CR-NA-CW	502	108	NA-CR-NA	502	109.9
H4-CW-NA	126	122.1	H5-CR-NA	126	125.7
CW-CW-H4	126	130.7			
CT-C-O2	335	116.21	O2-C-O2	356	124.97
H1-CT-C	243	109.50			
	Proper Torsion					
	K_ψ (kJ·mol^{-1}·rad^{-2})	γ (deg)	n		K_ψ (kJ·mol^{-1}·rad^{-2})	γ (deg)	n
NA-CR-NA-CW	50.21	180	2	NA-CR-NA-CN3	8.37	180	2
NA-CR-NA-CN2	8.37	180	2	H5-CR-NA-CW	6.28	180	2
H5-CR-NA-CN3	6.28	180	2	H5-CR-NA-CN2	6.28	180	2
CW-CW-NA-CN3	8.37	180	2	H4-CW-NA-CN3	6.28	180	2
CW-CW-NA-CR	50.21	180	2	CW-CW-NA-CN2	8.37	180	2
H4-CW-NA-CR	8.37	180	2	H4-CW-NA-CN2	6.28	180	2
NA-CW-CW-H4	6.28	180	2	NA-CW-CW-NA	50.21	180	2
H4-CW-CW-H4	6.28	180	2	HC-CT-CT-CN2	0.67	0	3
HC-CN2-CT-CT	0.67	0	3	HC-CN3-NA-CR	0.69	0	3
H1-CN2-CT-CT	0.67	0	3	CT2-CT-CT-CN2	4.39	0	3
CT2-CT-CT-CT	1.05	0	3	CN2-CT-CT-CT	1.05	0	3

CT-CT-CT-CT	1.05	0	3	HC-CT-CT-CT	0.67	0	3
HC-CT-CT-CT2	0.67	0	3	NA-CN2-CT-CT	4.39	0	3
NA-CN2-CT-HC	0.67	0	3	H1-CN2-CT-HC	0.63	0	3
HC-CN3-NA-CW	1.00	0	3	H1-CN3-NA-CR	0.69	0	3
H1-CN2-NA-CW	1.00	0	3	H1-CN2-NA-CR	0.69	0	3
CT-CN2-NA-CW	-0.74	0	1	CT-CN2-NA-CR	-0.99	0	1
HC-CT-CT-HC	0.63	0	3	HC-CN3-CT-HC	0.63	0	3
HC-CN3-CT-CT	0.67	0	3	H1-CT-C-O2	0	0	2
	Improper Torsion						
	K_ψ (kJ·mol^{-1}·rad^{-2})	γ (deg)	n		K_ψ (kJ·mol^{-1}·rad^{-2})	γ (deg)	n
NA-NA-CR-H5	4.60	180	2	CW-NA-CW-H4	4.60	180	2
CR-CW-NA-CN3	8.37	180	2	CR-CW-NA-CN2	8.37	180	2
CT-O2-C-O2	43.93	180	2				
	Van der Waals						
	r_i (Å)	ε_i (kJ/mol)			r_i (Å)	ε_i (kJ/mol)	
CR	1.908	0.3598		NA	1.824	0.7113	
CW	1.908	0.3598		H4	1.409	0.0628	
H5	1.359	0.0628		CT	1.908	0.4561	
CN3	1.907	0.7908		CN2	1.911	0.5941	
CT2	1.973	0.5565		H1	1.387	0.0669	
HC	1.487	0.0669		C	1.908	0.3598	
O2	1.661	0.8786					

Table S5 Heat of vaporization for the liquid-phase [C$_n$mim][OAc](n = 4, 6) ILs system simulated in this work and available experiments.

	U_{inter}/kJ·mol^{-1}	$U_{ionpair}$/kJ·mol^{-1}	$\Delta^g_l H^o_m$/kJ·mol^{-1}	$\Delta^g_l H^o_m$(exp.)/kJ·mol^{-1}
[C$_4$mim][OAc]	526.3331	394.5340	134.29	127.8 ± 4.3
[C$_6$mim][OAc]	534.8122	394.4713	142.84	133.1 ± 4.2